AGE-RELATED CHANGES IN THE MECHANICAL PROPERTIES OF ARTERIES

by

Kevin Scott Nye

A thesis submitted to the faculty of
The University of Utah
in partial fulfillment of the requirements for the degree of

Master of Science

Department of Mechanical Engineering

The University of Utah

May 2015

The University of Utah Graduate School

STATEMENT OF THESIS APPROVAL

The thesis of Kevin Scott Nye

has been approved by the following supervisory committee members:

Kenneth Monson	, Chair	10/10/2014 Date Approved
Brittany Coats	, Member	10/10/2014 Date Approved
Jeffrey Weiss	, Member	10/10/2014 Date Approved

and by Tim Ameel , Chair/Dean of

the Department/College/School of Mechanical Engineering

and by David B. Kieda, Dean of The Graduate School.

ABSTRACT

Brain injuries are devastating and complicated due to frequent, permanent side effects and varied symptomatic progressions. While brain injuries are damaging at any stage in life, they have far more tragic consequences in the early, developmental period. Brain injuries early on can result in neurodevelopmental disabilities, or even death. Because of the mechanical nature of brain injuries, damage to the cerebral vasculature is common; this consequence prompts the study of their loading behavior.

It is well known that human blood vessels develop throughout life and that development is particularly rapid during infancy. However, the mechanical properties of developing blood vessels remain largely undefined. Characterization of isolated blood vessels may shed great insight into the progression of brain injuries.

Two types of vessels were studied to identify age-related changes in mechanical properties: human umbilical artery and ovine middle cerebral artery. In the umbilical artery study, we hypothesized that vessels from a younger gestational age would be less stiff and indicate susceptibility to intraventricular hemorrhage (IVH), a common type of brain injury in preterm infants. Single umbilical arteries were dissected from cord segments collected from births between 24 and 40 weeks. Axial and circumferential strips were taken from artery segments and subjected to uniaxial loading. Umbilical artery properties were not shown to significantly change in either the axial or circumferential directions across the 24–40 week gestation, nor indicate IV susceptibility.

Traumatic brain injury often results in vascular damage and dysfunction. As a result, these injuries have devastating consequences, especially in the pediatric population. Consequently, it is important to understand the specific loading behavior of young, compared to adult, cerebral vessels. In the ovine cerebral artery study, we hypothesized younger vessels would be less stiff and more distensible compared to older vessels. Whole cerebral arteries were taken from the preterm, or fetal, lambs (~132 days gestation in sheep) up through adult (37 years) and subjected to biaxial loading tests. Our findings show significant differences in mechanical properties between younger compared to older ovine cerebral vessels. Differences in mechanical properties between young and older cerebral vessels would likely result in distinct loading behaviors and subsequent levels of damage and dysfunction.

As blood vessels develop and grow, their mechanical characteristics can significantly change. Age-related differences in the mechanical properties of vessels should be considered when developing injury or disease models and diagnostic or treatment regimes.

TABLE OF CONTENTS

LIST OF FIGURES

ACKNOWLEDGMENTS

The development of this work would not be possible without funding or special assistance from a number of sources. An interdisciplinary seed grant from the University of Utah funded a portion of this work, and collaborations with Dr. Sean Esplin at Intermountain Medical Center and the Albertine lab in the Pediatrics department, neonatology division at the University of Utah, provided invaluable assistance and materials. Also, the optimism, patience, and help from Ken Monson made this work possible.

CHAPTER 1

PURPOSE/BACKGROUND

Purpose

The purpose of this work was to explore age-related changes in mechanical properties of arteries with the aim to improve understanding of cerebral injuries in the pediatric population. Described more thoroughly in Chapter 2, a devastating brain injury common to preterm and low birth weight infants is hemorrhaging in the ventricles of the brain, termed intraventricular hemorrhage or IVH. Occurrences of IVH increase at earlier gestational ages and are thought to be a result of structural deficiencies in the infant vasculature. The first part of this work explores age-related changes in the mechanical properties of the umbilical artery as they relate to gestational age and occurrence of IVH. Although not expected to have mechanical properties similar to intracranial arteries, umbilical vessels develop concurrently with the infant vasculature and are more available than intracranial arteries. Characterizing umbilical artery mechanical properties may reveal structural deficiencies responsible for IVH.

Traumatic brain injury, or TBI, is an especially devastating disease in the pediatric population and carries with it with frequent, long-lasting side effects. Damage to the cerebral vasculature coincides with TBI, and understanding tissue level loading behavior as it relates to age of cerebral arteries is an important step in better understanding the injury. The second part of this work, presented in Chapter 3, explores

the age-related changes in the mechanical properties of the cerebral vasculature of sheep from a fetal age up to adulthood. The chapter explores the mechanical properties of the young, developing vasculature as it compares to adults. Understanding age-related properties may shed insight into the marked differences in symptoms of young compared to older TBI victims.

The Circulatory System

The human circulatory system is the means by which blood, nutrients, and oxygen circulate to the individual tissues of the body. Alternatively, it serves to collect and remove accumulated carbon dioxide and cellular wastes. This system also plays a major role in regulating blood pressure, body temperature, delivering signaling hormones and components of the immune system, and carrying clotting factors [1]. The vessels of the circulatory system extend into every small space in the body such that nearly all the cells are within 0.1 mm of a vessel [2]. These vessels are capable of rapid, dynamic change to maintain homeostasis and are continuously developing throughout the human lifetime. Because the circulatory system plays such a vital role in the body, damage or disease can be devastating. Loss of blood, aneurysm, contusion, edema, thrombosis, and embolism are all potentially harmful consequences from damage to vessels of the circulatory system.

The Conducting Vessels

The specific function and wall constituents of a vessel define it as either an artery or a vein. Arteries generally carry oxygenated blood and nutrients to the tissue level capillary beds, while veins carry deoxygenated blood and cellular wastes away from

them. The conducting vessels of the circulatory system share similar structural and cellular components; however, the proportions of these components are distinct in both arteries and veins. Arteries are generally thicker and more elastic and have a greater abundance of smooth muscle cells than similar sized veins [1]. These properties make arteries well-suited for their role of attenuating pressure oscillations of the heart, forcing blood into smaller diameter conducting vessels, and regulating blood flow and pressure to specific regions of the body. Veins are generally more extensible and have a thinner wall compared to similar sized arteries [1]. This structure allows them to act as a low-pressure reservoir for blood. The characteristics of arteries and veins make them perfectly suited for their specific roles in the body.

Three layers constitute the majority of blood vessels: tunica intima, tunica media, and tunica adventitia. The innermost layer of the intima, directly in contact with the blood, is comprised of a single layer of longitudinally oriented endothelial cells called the endothelium. This layer serves a significant role in the body in transmitting signaling hormones, secreting vasoactive compounds, and regulating nutrient absorption; this layer is found in all blood vessels. The media lies between the intima and the adventitia and is generally composed of helically oriented layers of smooth muscle cells surrounded by collagen and elastin fibers [3]. The adventitia is the outermost layer and is comprised of primarily collagen, with some elastin, nerves, and fibroblasts. It is the collagen component of the adventitial layer that is responsible for the maximum stiffness of blood vessels [4].

Blood Vessel Development

Blood vessels develop throughout their existence by a complex sequence of genetic expressions and coordination of enzymes [4]. This continuous developmental schema serves to establish a structure that is optimized for its specific function and loading conditions. In humans, blood vessels develop in the 3rd week of gestation. During this week, blood islands, which serve as the base for a primitive circulatory network, form within the embryo. Angioblasts then join with the blood islands to form vessels; soon thereafter, blood begins to circulate within them.

Over the gestational period, immature perivascular cells continue to invade the primitive vascular network. Depending on the location and loading conditions within the circulatory system, these perivascular cells begin to differentiate into smooth muscle or pericytes. As the neonate continues to grow, an increase in the diameter of blood vessels occurs in response to increases in pressure and flow. In the arterial system, the media layer begins to thicken, and the collagen content begins to increase; at the same time, perivascular cells decrease. After birth, the opening and development of the lungs cause changes in flows and pressures in the infant circulatory system that induce further growth in the vasculature structures. Blood vessels continue to develop into adulthood with changes such as increases in collagen to elastin ratios, morphology, and stiffening [3,4].

Structural Components of Blood Vessels

Collagen, elastin, and smooth muscle cells are three components of blood vessels that contribute to its overall structure [3]. Elastin fibers generally govern low-level loading, and the collagen fibers dominate at higher level loading. The heterogeneous mixtures and orientations of these components are largely dictated by the specific

function and location of the vessel in the body. The orientation and arrangement of these structural components makes blood vessels an anisotropic material, meaning the loading behavior is dependent on the direction of the applied load.

The mechanical properties of blood vessels are dynamic and are altered by a number of factors including changes in blood pressure and flow rate, body temperature, and responses to signaling hormones [2]. Generally, vessels in the body are in an active state, or one in which the smooth muscle component is slightly contracted, called smooth muscle tone. Alternatively, a passive state is one in which there is an absence of smooth muscle tone. Identifying the loading behavior of both the active and passive states is important in developing an overall picture of the mechanics of blood vessels. A number of factors, including age and vascular diseases, chronically affect both active and passive states of blood vessels [3].

Generally, it has been shown that advancing age leads to stiffer blood vessels; these alterations are due to changes in proportions of structural and cellular components [5]. Busby and Burton showed younger human cerebral vessels to be more distensible than older cerebral vessels [6]. Cox showed a similar trend of increasing stiffness in the rat carotid artery with age, as a result of changes in collagen and elastin ratios [7]. Goyal et al. showed changes in the collagen, elastin, and smooth muscle components of the ovine MCA during the prenatal period [8]. However, the loading behavior of preterm or fetal arteries remains ill defined. The potential to create a complete relationship between age and loading behavior of blood vessels still exists and could greatly enhance the understanding of vascular diseases or injury throughout all stages of life.

References

[1] Randall, D. J., Burggren, W. W., French, K., and Eckert, R. A. p., 2002, Eckert Animal physiology : mechanisms and adaptations, W.H. Freeman and Co., New York.

[2] Silverthorn, D. U., 2010, Human physiology : an integrated approach, Pearson, San Francisco, CA.

[3] Humphrey, J. D., 1995, "Mechanics of the arterial wall: review and directions," Crit. Rev. Biomed. Eng., 23(1–2), pp. 1–162.

[4] Dobrin, P. B., 1978, "Mechanical properties of arteries," Physiol. Rev., 58(2), pp. 397–460.

[5] Busby, D. E., and Burton, A. C., 1965, "The effect of age on the elasticity of the major brain arteries," Can. J. Physiol. Pharmacol., 43, pp. 185¬202.

[6] Cox, R. H., 1977, "Effects of age on the mechanical properties of rat carotid artery," Am. J. Physiol., 233(2), pp. H256¬263.

[8] Goyal, R., Henderson, D. A., Chu, N., and Longo, L. D., 2012, "Ovine middle cerebral artery characterization and quantification of ultrastructure and other features: changes with development," Am. J. Physiol. Regul. Integr. Comp. Physiol., 302(4), pp. R433–445.

CHAPTER 2

UMBILICAL CORD ARTERY MECHANICAL PROPERTIES AT VARIOUS GESTATIONAL AGES

Kevin S. Nye, M. Sean Esplin, Kenneth L. Monson, Umbilical Cord Artery Mechanical Properties at Various Gestational Ages, American Journal of Perinatology, (ahead of print), Thieme, www.thieme.com (reprinted by permission).

Original Article

Umbilical Cord Artery Mechanical Properties at Various Gestational Ages

Kevin S. Nye, BS[1] M Sean Esplin, MD[2,3] Kenneth L. Monson, PhD[1,4]

[1] Department of Mechanical Engineering, University of Utah, Salt Lake City, Utah
[2] Division of Maternal Fetal Medicine, Department of Obstetrics and Gynecology, University of Utah, Salt Lake City, Utah
[3] Department of Obstetrics and Gynecology, Intermountain Health Care, Salt Lake City, Utah
[4] Department of Bioengineering, University of Utah, Salt Lake City, Utah

Address for correspondence Kenneth L. Monson, PhD, Department of Mechanical Engineering, University of Utah, 50 S. Central Campus Dr., MEB 2132, Salt Lake City, UT 84112 (e-mail: ken.monson@utah.edu).

Am J Perinatol

Abstract

Objective Umbilical cord tissue is naturally available after birth and may provide insight into the health of a newborn. Intraventricular hemorrhage (IVH) is a common complication of prematurity that is suspected to be associated with structural deficiency of the vasculature. We are interested in determining whether umbilical vessel properties could be used to indicate increased risk for IVH. As a first step toward this, we investigated umbilical artery properties as a function of gestational age.

Study Design A total of 31 umbilical cord specimens were collected from births ranging from 24 to 40 weeks gestation. Specimens were grouped according to gestational age (less than 25, 26–30, 31–35, and 36–40 weeks). Tension tests were performed on axial and circumferential strips obtained from umbilical arteries. Stiffness, corresponding stretch values, and cross-sectional tissue areas were compared using analysis of variance.

Results Stress-stretch curves displayed no apparent differences across the gestational age range. Statistical analysis of stiffness and stretch values suggested no differences between groups ($p > 0.05$). Significance was shown between cross-sectional areas of some groups.

Conclusions Mechanical characterization of umbilical arteries suggests that no significant changes in material properties occur in the range of 24 to 40 week gestational age.

Keywords
- umbilical artery
- mechanical properties
- intraventricular hemorrhage
- neonate

Premature and very low-birth-weight infants are susceptible to numerous injuries during and after parturition. If these injuries are neurological in nature, they can result in long-term cognitive and motor skill deficiencies. Intraventricular hemorrhage (IVH), bleeding in the ventricle region of the brain, is a common complication of prematurity and occurs in 32% of infants with birth weights less than 1,500 g and born before 32 weeks gestation[1]; 75% of these will experience long-term neurological disabilities.[2] Structural deficiencies in the developing cerebral vasculature are suspected to underlie the high incidence of IVH,[3–5] though this has not been confirmed.

While tissue specimens are generally difficult to obtain from neonates, a portion of the infant circulation becomes available at birth through the umbilical cord. The composition and morphology of the umbilical cord has been studied and linked with maternal and fetal diseases[6] and with anthropomorphic parameters.[7] For example, umbilical cord material properties have been shown to change in the intrauterine growth restriction

received
March 13, 2014
accepted after revision
May 14, 2014

DOI http://dx.doi.org/10.1055/s-0034-1383850.
ISSN 0735-1631.

lamb model.[8] These findings suggest that the umbilical cord is influenced by fetal health and therefore could potentially be used to predict susceptibility to disease or injury. Because of the limited information on correlations between umbilical cord material properties and infant health, a full understanding of its prognostic value has not been achieved.[9]

To better understand vascular instability during development, especially as it may apply to IVH, the objective of this study was to define the mechanical response of umbilical arteries as a function of gestational age. Although, umbilical and cerebral vessels are expected to have different properties, any systemic changes evident in umbilical arteries may be relevant to cerebral vessels. Preliminary work in our laboratory shows that defining the properties of whole umbilical cord artery is complicated by the natural helical structure of the vessels. As a result, we here report the results from tension tests on axial and circumferential strips of human umbilical cord artery from infants of various gestational ages.

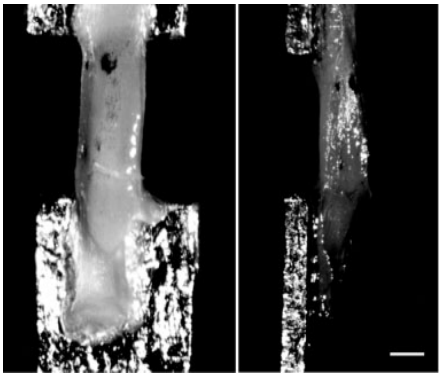

Fig. 1 Front and side views of an axial umbilical artery strip mounted in the uniaxial tension tester. The luminal sides of the artery strips were adhered to stainless steel plates with cyanoacrylate glue. In some cases (including that shown), small black microspheres were applied to the abluminal side to enable tracking of tissue motion. Scale bar is 1 mm.

Methods

Tissue Acquisition and Preparation

Specimens were collected from normal umbilical cords following births with 24 to 40 weeks of gestation at Intermountain Medical Center in Murray, Utah (IRB no. 1014329). Samples were 5 cm long and were taken approximately 3 cm from the placental insertion site. The cord segments were placed in 0.9% saline solution and kept in a cold refrigerator until they were retrieved and transported to the laboratory for testing. All specimens were transported to the University of Utah on ice and tested within 24 hours of parturition.[10] Upon arrival to the laboratory, cord samples were placed in a dish containing cold, calcium free, phosphate buffered saline (PBS); lack of calcium precluded smooth muscle contraction during tests.

Vessels were dissected by inserting the tip of a pair of microscissors between the artery and the surrounding Wharton jelly and making an incision through the jelly along the path of the artery. Tissue forceps were used to hold the end of the artery, while the connective tissue surrounding the artery was cut away with microscissors.

Once the surrounding tissue was removed, cross-sections and axial and circumferential strips were cut from the dissected vessels; both axial and circumferential strips were cut at the same width (1.736 mm), using a prefabricated cutter, at lengths between 3 and 5 mm for circumferential strips and 8 and 10 mm for axial strips.

Experimental Setup and Procedure

To prepare each specimen for testing, it was removed from the PBS bath and excess fluid was wicked away with a low-lint wipe. The luminal side of each end was then placed onto a 5 mm × 5 mm × 1.59 mm stainless steel plate with a small amount of cyanoacrylate glue covering its surface (►**Fig. 1**). The stainless steel plates were fixed to 18 gauge needle lures, which were tightened into prefabricated acrylic blocks built to interface with our vessel testing system.[11] An adjustable support arm was used to fix the distance between the two acrylic blocks during specimen attachment; it was removed once the blocks were attached to the testing fixture. A 1,000 g capacity load cell (Model 31 Low, Honeywell, Golden Valley, MN) was mounted in line with the specimen. Stretching of the tissue specimen was performed at a rate of 0.1 mm/s with either a voice coil actuator (MGV52–25–1.0, Akribis, Sunnyvale, CA) or a custom linear stage (Parker Automation, Cleveland, OH) driven by a stepper motor (H-2222–3, Intelligent Motion Systems, Marlborough, CT). A digital camera (PL-A641, Pixelink, Ottawa, Canada) with a high magnification lens (VZM 450i, Edmund Optics, Barrington, NJ) captured side view images of specimens during testing. Test control as well as data and image acquisition were accomplished using a LabVIEW (National Instruments, Austin, TX) program written by our group. Transducer and video data were acquired at 100 and 3 Hz, respectively.

Once the specimen was attached to the testing machine and the support arm was removed, the estimated specimen reference length was obtained by stretching the vessel strip from an unloaded (slightly buckled) state to a stretched state in 0.1 mm increments. Stretch increments were applied to the specimen until a slight increase in force was observed, at which point the specimen was unstretched 0.1 mm and the distance between the steel plate ends was taken as the estimated reference length. During testing, PBS was periodically dripped onto the specimen to prevent dehydration. The strips were then preconditioned between 1 and 1.2 times the estimated specimen reference length through 7 cycles at a rate of 0.1 mm/s. Given that stretch values over 2.0 were commonly observed in the subsequent failure tests, a stretch level of 1.2 times the estimated reference length was deemed to be reasonable for basic preconditioning. Following the preconditioning cycles, the specimen was stretched from a relaxed state to failure, or until it detached from the plates.

Data Processing

Failure test data were processed to calculate the overall stress–stretch response. Specimen reference length (l_0) was

defined as the distance between two natural fiducial markers in the specimen midsection. Its value was determined from an image at the beginning of the test corresponding with a tare load value of 0.0035 N. The distance between these two fiducial markers was measured in six additional, equally spaced images, up to 60 kPa in axial specimens and 30 kPa in circumferential specimens. The ratio of the distance between the markers in each image (l_i) and the reference length (l_0) was defined as the stretch ratio (λ). The calculated stretch values were observed to increase linearly with time, so a line was fit to the seven evaluated points. Intermediate stretch values were defined through interpolation to provide a one-to-one relationship with the stress data. First Piola–Kirchhoff stress (P) was calculated as the measured force (F_i) divided by the reference cross-sectional area (Eq. 1),

$$P = \frac{F_i}{t_0 w_0}$$

where, w_0 is the unstretched specimen width and t_0 is the unstretched specimen thickness; t_0 was measured from the image corresponding to l_0.

The resulting stress–stretch curves were characterized by quantifying both stiffness and stretch at two levels of stress. Specimen stiffness was defined as the slope of the stress–stretch curve at stress values of 40 and 20 kPa for axial specimens and of 20 and 10 kPa for circumferential specimens. These particular stress values were chosen because all stress–stretch curves passed through them before the occurrence of any failure or slippage of specimens. The selected stress values also correspond well with estimated in vivo stresses. The stretch ratio associated with each stress level was also recorded.

Images of umbilical artery cross-sections were taken using a microscope (Stemi 200-C, Zeiss, Thornwood, NY) with an attached digital camera (PL-A662, Pixelinx, Ottawa, Canada). Binary images of the inner and outer areas of the vessel cross-section were created in MATLAB (MathWorks, Natick, MA) using the function "roipoly." Outer and inner binary images were added to obtain a single binary image of the vessel cross-section. Cross-sectional area was then calculated by summing the total number of pixels in the binary image and multiplying by the determined conversion factor.

Statistical Analysis

Umbilical samples were grouped into four gestational age ranges (in weeks): 36 to 40, 31 to 35, 26 to 30, and 25 or less (LTE25). One-way analysis of variance (ANOVA) was performed to evaluate the significance of gestational age on measured stiffness and stretch values and on cross-sectional area. The significance of material direction was also explored. Post hoc *t*-tests, using a Bonferroni correction factor, were performed where ANOVA indicated significance. Linear regression was also used to evaluate the influence of age on the measured values. In all cases, $p \leq 0.05$ was considered significant. The statistical analysis of the data was performed using StatPlus (Analystsoft Inc., Vancouver, Canada).

Results

A total of 31 umbilical cord specimens were obtained (►**Table 1**); six (all born at less than 32 weeks gestation) of the donors went on to experience some form of IVH. Handling of the cord samples suggested that those at later gestational ages were less compliant and denser than earlier samples. Arteries from later gestational ages were also generally easier to dissect compared with earlier vessels because of weaker adherence to the surrounding Wharton jelly. Although not quantified, vessels (and cords) from older infants tended to be more coiled than those from earlier births.

Table 1 Axial and circumferential stiffness and corresponding stretch values at stress levels of 20 and 40 kPa and 10 and 20 kPa, respectively, along with *p* values calculated for ANOVA and linreg

Stress level (kPa)	Gestational age (wks)				*p*-Value	
	LTE25 ($n = 5$)	26–30 ($n = 7$)	31–35 ($n = 11$)	36–40 ($n = 8$; 7[a])	ANOVA	linreg
Stiffness (kPa)						
Axial (40)	285.10 ± 197.16	148.68 ± 66.58	181.96 ± 64.10	217.45 ± 68.83	0.1198	0.5291
Axial (20)	153.36 ± 71.45	94.39 ± 32.90	119.39 ± 31.15	147.38 ± 61.63	0.1214	0.7367
Circ (20)	57.89 ± 11.59	55.51 ± 23.68	76.53 ± 47.80	80.83 ± 73.33[a]	0.6776	0.1490
Circ (10)	58.63 ± 22.76	51.26 ± 26.83	57.81 ± 38.46	58.29 ± 38.69	0.9736	0.5370
Stretch						
Axial (40)	1.33 ± 0.11	1.52 ± 0.20	1.39 ± 0.09	1.41 ± 0.17	0.1728	0.8984
Axial (20)	1.21 ± 0.07	1.32 ± 0.15	1.24 ± 0.07	1.29 ± 0.18	0.2382	0.6258
Circ (20)	1.34 ± 0.12	1.50 ± 0.28	1.44 ± 0.24	1.62 ± 0.44	0.4290	0.3341
Circ (10)	1.15 ± 0.08	1.27 ± 0.18	1.23 ± 0.16	1.33 ± 0.23	0.3416	0.2430

Abbreviations: ANOVA, analysis of variance; linreg, linear regression.
[a]The stress-stretch curve of one circumferential 36-40 week specimen did not reach 20 kPa; therefore the sample size was 7 instead of 8.

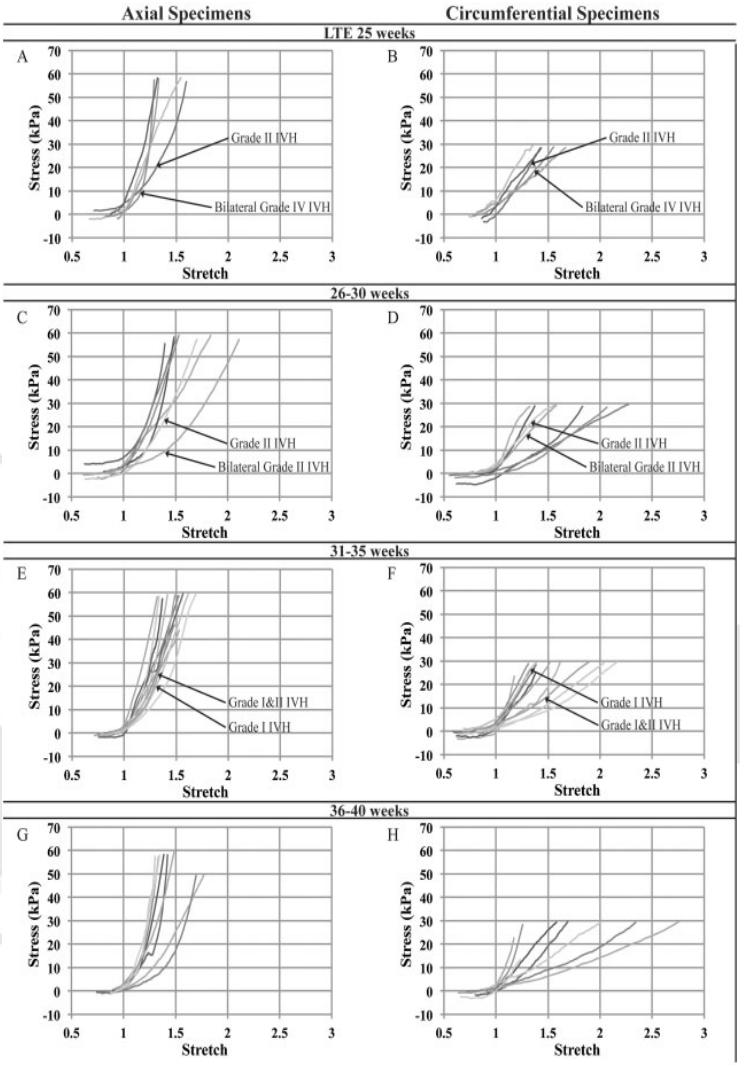

Fig. 2 Stress–stretch curves of umbilical artery specimens. Axial (A, C, E, G) and circumferential (B, D, F, H) specimens from LTE25 (A, B), 26 to 30 (C, D), 31 to 35 (E, F) and 36 to 40 (G, H) week groups. Curves from infants that experienced IVH (grades I to IV; some bilateral) are annotated. IVH, intraventricular hemorrhage.

The stress–stretch curves of both the axial and the circumferential specimens under uniaxial tension were generally nonlinear (►**Fig. 2**), similar to other soft tissues. Data from each test are presented up to the maximum stress value to which fiducial markers were tracked. Although, failure of the specimens was not achieved in many cases due to premature detachment from the loading plates, each specimen was stretched well beyond typical in vivo loading values (often to multiple times their unloaded length before failure; data not shown). As is common for biological tissue, there was significant scatter within each group. There were no obvious differences between curves as a function of gestational age, but circumferential specimens tended to be more extensible than axial strips. Stress–stretch curves from the small number of infants that did experience IVH demonstrated no apparent differences from those that did not, though numbers were small.

Mean stiffness values of both axial and circumferential specimens are summarized by gestational age in ►**Fig. 3**. Consistent with observations of the stress–stretch plots, one-way ANOVA demonstrated no statistical significance of gestational age in stiffness for either the axial ($p = 0.12$ at 40 kPa and $p = 0.12$ at 20 kPa) or circumferential ($p = 0.68$ at 20 kPa and $p = 0.97$ at 10 kPa) direction. Linear regression of stiffness versus gestational age produced similarly high p values (►**Table 1**).

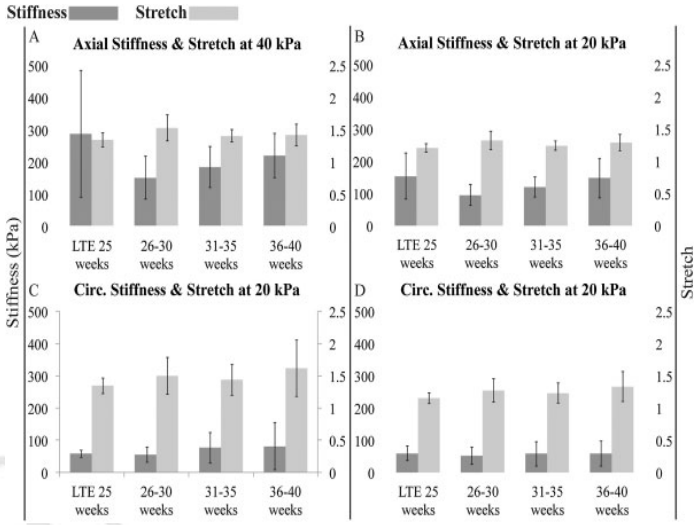

Fig. 3 Mean axial stiffness and stretch values evaluated at (A) 40 and (C) 20 kPa and mean circumferential stiffness and stretch values evaluated at (B) 20 and (D) 10 kPa.

Mean stretch ratios at the evaluated stress levels are also summarized in ►**Fig. 3**. As with specimen stiffness, age did not have a statistically significant effect on either axial ($p = 0.16$ at 40 kPa and $p = 0.24$ at 20 kPa) or circumferential ($p = 0.43$ at 20 kPa and $p = 0.34$ at 10 kPa) stretch. Of note, linear regression of stretch versus gestational age demonstrated a positive slope, but the trend was not statistically significant (►**Table 1**).

In measurements corresponding to the same umbilical artery, it was possible to evaluate differences between material directions at 20 kPa (►**Table 2**). Results show that specimens were, on average, 2.45 times stiffer and 0.88 times less extensible axially than circumferentially, with no apparent trend in these relationships with age.

As expected, the mean cross-sectional area of umbilical arteries increased with gestational age (►**Fig. 4**). ANVOA performed between groups indicated significance ($p = 0.004$), and post hoc testing showed significance between LTE25 and the 31 to 35 and the 36 to 40 week groups ($p = 0.002$ and 0.001, respectively). Typical unloaded outer diameter and wall thickness measurements increased from about 1.0 to 2.3 mm and from 0.3 to 0.9 mm, respectively, from LTE25 to term.

Discussion

The objective of this research was to investigate the effect of gestational age on the mechanical properties of umbilical cord arteries. While earlier cord samples were qualitatively different from later samples in size and coiling, results from experiments show that artery mechanical properties did not change significantly with gestational age.

The finding that properties did not change with age was unexpected. This was especially true given the observation that cross-sectional area, as well as gross cord features such as apparent compliance and coiling, did change with age. Others have also reported changing blood flow rates over the same period.[12] Regardless, our findings suggest that the remodeling and growth processes in these vessels occur in such a way as to maintain a consistent mechanical response.

The observed greater stiffness in the axial, compared with the circumferential, direction of loading is notable. It is important to state that the natural curvature of circumferential specimens made identification of the reference length more challenging and possibly led to overprediction of stretch values in this direction. However, this influence

Table 2 Ratios of axial to circumferential stiffness (stif ratio) and stretch (str ratio) determined at 20 kPa, along with *p* values from ANOVA and linear regression evaluating directional differences between ratios within the same age group

	Gestational age (wks)				*p*-Value	
	LTE25	26–30	31–35	36–40	ANOVA	linreg
stif ratio	2.88 ± 1.74	2.07 ± 1.28	2.13 ± 1.34	3.04 ± 2.03	0.5365	0.9669
str ratio	0.90 ± 0.08	0.92 ± 0.22	0.88 ± 0.13	0.83 ± 0.17	0.7883	0.5535

Abbreviation: ANOVA, analysis of variance.

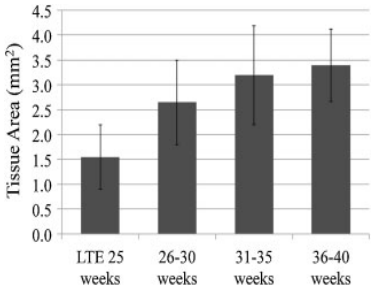

Fig. 4 Cross-sectional tissue areas of umbilical arteries. At 36 to 40 weeks 3.39 ± 0.73 mm^2 ($n = 8$), 31 to 35 weeks 3.19 ± 1.00 mm^2 ($n = 12$), 26 to 30 weeks 2.64 ± 0.85 mm^2 ($n = 7$), and LTE25 weeks 1.54 ± 0.65 mm^2 ($n = 5$). LTE25, less than 25 week gestational age.

was not so dramatic that it would have significantly changed conclusions regarding the relative stiffness. Functionally, the cord arteries experience consistent loading from blood pressure and flow; these loads are likely influential in vessel development, with the primary need being to accommodate circumferential loading. However, other tensile and compressive loads also occur as the fetus moves relatively freely within the uterus. The coiled nature of the cord likely helps minimize any severe longitudinal stretching of the cord material under these conditions, allowing for a greater stiffness of the material in the commonly unloaded axial direction.

A primary motivation for this study was to investigate any changes in umbilical vessel integrity with gestational age, as a possible reflection of intracranial vessel development and the incidence of IVH. It is important to note that our findings are limited to the umbilical artery and may or may not apply to intracranial vessels. This question needs to be addressed more directly. On a related note, during the course of this study, a small number of the cord samples collected were from infants that went on to experience some grade of IVH. While these cases were too limited (six cases) to draw any firm conclusions, there was no apparent difference in their artery properties, suggesting that cord artery mechanical properties are likely not an effective predictor of IVH susceptibility. However, further exploration of cord mechanical properties and other pathological conditions that affect fetus and infant health, including cord abnormalities, may lend to more positive correlations.

While the presented results are considered reliable, some methodological limitations should be noted. First, we assumed that uniaxial tests would provide sufficient information to draw conclusions on any change in artery properties with gestational age. We have previously conducted biaxial tests of intact vessels to explore their response,[11] but the natural coiled structure of the umbilical arteries prevents direct study of pure material properties in the intact configuration. While biaxial tests provide significantly greater ability to explore mechanical behavior, there is little reason to expect that gestational age would be found to have a more significant response in biaxial tests than in uniaxial experiments. Another limitation to our study design was the bonding of samples on only the luminal side, potentially leading to nonuniform stretch through the specimen thickness. However, application of the cyanoacrylate tended to secure both the luminal and abluminal sides such that the whole of the tissue adjacent to the plate was hard to the touch. This appeared to help reduce any nonuniformity; analysis of microsphere displacement on the abluminal side of one specimen resulted in a difference of less than 10% between luminal and abluminal stretch ratios. Another methodological consideration is the use of a calcium-free solution in these tests. Without this, contributions from smooth muscle would likely have influenced our findings, especially in the circumferential direction. It has been shown that contractility of umbilical vessels is altered by factors such as diabetes, smoking,[13] and arterial flow velocity,[14] so smooth muscle behavior appears to have prognostic value in some conditions. However, the use of calcium-free solution in the present study was necessary to allow isolated study of passive vessel response.

Acknowledgment

Funding for this study was provided by an interdisciplinary seed grant from the University of Utah.

References

1 Lemons JA, Bauer CR, Oh W, et al; NICHD Neonatal Research Network. Very low birth weight outcomes of the National Institute of Child health and human development neonatal research network, January 1995 through December 1996. Pediatrics 2001; 107(1):E1

2 McCrea HJ, Ment LR. The diagnosis, management, and postnatal prevention of intraventricular hemorrhage in the preterm neonate. Clin Perinatol 2008;35(4):777–792, vii

3 Ghazi-Birry HS, Brown WR, Moody DM, Challa VR, Block SM, Reboussin DM. Human germinal matrix: venous origin of hemorrhage and vascular characteristics. AJNR Am J Neuroradiol 1997; 18(2):219–229

4 Gould SJ, Howard S. An immunohistochemical study of the germinal layer in the late gestation human fetal brain. Neuropathol Appl Neurobiol 1987;13(6):421–437

5 Grunnet ML. Morphometry of blood vessels in the cortex and germinal plate of premature neonates. Pediatr Neurol 1989;5(1): 12–16

6 Di Naro E, Ghezzi F, Raio L, Franchi M, D'Addario V. Umbilical cord morphology and pregnancy outcome. Eur J Obstet Gynecol Reprod Biol 2001;96(2):150–157

7 Raio L, Ghezzi F, Di Naro E, et al. Sonographic measurement of the umbilical cord and fetal anthropometric parameters. Eur J Obstet Gynecol Reprod Biol 1999;83(2):131–135

8 Dodson RB, Rozance PJ, Fleenor BS, et al. Increased arterial stiffness and extracellular matrix reorganization in intrauterine growth-restricted fetal sheep. Pediatr Res 2013;73(2):147–154

9 Ferguson VL, Dodson RB. Bioengineering aspects of the umbilical cord. Eur J Obstet Gynecol Reprod Biol 2009;144(Suppl 1): S108–S113

10 Stemper BD, Yoganandan N, Stineman MR, Gennarelli TA, Baisden JL, Pintar FA. Mechanics of fresh, refrigerated, and frozen arterial tissue. J Surg Res 2007;139(2):236–242

11 Bell ED, Kunjir RS, Monson KL. Biaxial and failure properties of passive rat middle cerebral arteries. J Biomech 2013;46(1):91–96
12 Barbera A, Galan HL, Ferrazzi E, et al. Relationship of umbilical vein blood flow to growth parameters in the human fetus. Am J Obstet Gynecol 1999;181(1):174–179
13 Wang Y, Zhao SJ. Vascular Biology of the Placenta. San Rafael: Morgan & Claypool Sciences; 2010
14 Giles W, O'Callaghan S, Read M, Gude N, King R, Brennecke S. Placental nitric oxide synthase activity and abnormal umbilical artery flow velocity waveforms. Obstet Gynecol 1997;89(1):49–52

CHAPTER 3

AGE EFFECTS IN SHEEP CEREBRAL ARTERY MECHANICAL PROPERTIES

Introduction

Traumatic brain injury (TBI) in the pediatric population is responsible for over 400,000 emergency department visits, 29,000 hospitalizations, and over 3,000 deaths each year in the United States [1], with annual care costs estimated at $60 billion [2]. Life-long neurological handicaps commonly result, making these injuries especially devastating to the pediatric population. Additionally, the consequences of TBI are markedly different in children compared to adults. Contusions in infants are distinct from those in the adult brain; they manifest as tears in the cerebral white matter and in the outer layers of the cortex rather than as hemorrhage and necrosis [3]. Also, cerebral blood flow (CBF) and autoregulation are commonly disturbed following TBI, but the response in children can be markedly different from, and more variable than, that of adults [4–8]. Uncontrollable brain swelling due to an increase in cerebrovascular volume and CBF is another unique feature of pediatric response to TBI [9–11].

Because TBI is initiated by mechanical loading, determining tissue-level load response is an important step in understanding the disease. Cerebral blood vessels are frequently damaged as part of head trauma in both children and adults, leading to hemorrhage and other vascular dysfunction [12]. We have previously investigatedthe properties of human adult cerebral arteries [13–15]. However, thresholds for cerebral

vascular damage in both adults and children remain poorly defined. We hypothesized that the passive mechanical properties of cerebral arteries, both at subfailure and failure levels, are age dependent. Specifically, we anticipated that younger vessels would be more extensible but carry less stress at similar stretch levels than those from older animals. We investigated our hypothesis using a sheep model in four age groups: fetal, newborn, juvenile, and adult. Defining age-dependent properties of cerebral vessels is critical to better define thresholds for pediatric TBI and may also lend insight into the unique response to TBI seen in children.

Methods

Tissue Collection/Preparation

Ovine middle cerebral arteries (MCAs) were collected from animals ranging in age from fetal to adult. In some cases, both left and right MCAs from the same animal were tested. In total, 11 MCAs each were tested from nine fetal lambs (~132 days gestation; 88% full gestation), six newborn lambs (8 days old, full term or 150 days gestation), six juvenile lambs (3–7 months), and 10 adult ewes (3–7 years). All the fetal, all but one adult, and four juvenile vessels were obtained from the Pediatric-Neonatology lab at the University of Utah; the remaining specimens were collected from local slaughterhouses. Ovine MCAs were removed shortly after death and placed in cold, calcium-free, phosphate-buffered saline (PBS; KH_2PO_4 1.54, NaCl 155.2, Na_2HPO_4-$7H_2O$ 2.7; concentrations in mM). Vessel testing always occurred within 48 hours of death; Stemper et al. has shown no significant differences in properties between tissues refrigerated at 24 and 48 hours [16]. In most cases, animals were sacrificed with an injection of beuthanasia, but some older animals were sacrificed by either electric or

percussion stunning. In the latter cases, the impact site was located away from the Circle of Willis to prevent damage to the MCAs prior to testing.

Following death, the head of the animal was removed and the top of the skull was cut away with a hacksaw and needle-nosed pliers. The brain was then freed from attachments to the inner surface of the skull, and the upper cervical portion of the spinal cord was severed using a scalpel. The brain was carefully separated from the dura such that MCAs were not disrupted. Removed ovine brains were then placed in a petri dish, and a proximal portion of MCA, with some of the underlying tissue, was removed with microscissors and placed in cold PBS. Under a dissecting microscope, pia and arachnoid layers were peeled away from the MCA with forceps. The vessel was then lifted away from the brain tissue with forceps while cutting penetrating vessels and other branches with microscissors. An approximately 8-mm long segment of vessel was removed, and branches were ligated using unwound 6-0 silk sutures. Cross sections were typically obtained from the proximal end of the dissected vessel and then photographed for cross section measurements.

Mechanical Testing

Mechanical tests were performed following previously established procedures [15,17]. In brief, prepared MCAs were mounted by ligating their ends onto grooved, 22-gauge needles using 6-0 silk sutures. The vessel was further secured by applying a small amount of cyanoacrylate glue to the ends after removing the surrounding fluid with a low-lint wipe; the suture also acted as a barrier to glue seepage. Testing was carried out using a custom load frame interfaced with a control and data collection program (LabVIEW, National Instruments, Austin, TX). Axial displacement was conducted using

either a custom linear stage (Parker Automation, Cleveland, OH) or a voice coil (MGV52-25-1.0, Akribis, Singapore), while force was measured with an inline, small-capacity load cell (Model 31 Low, 250 or 1000 g Honeywell, Golden Valley, MN). Grooved needles were placed onto open channels connected to a saline-filled syringe whose plunger was attached to a linear actuator (D-A0.25-ABHT17075-4-P, Ultra Motion, Cutchogue, NY). Internal pressure was measured with inline pressure sensors (26PCDFM6G, Honeywell, Golden Valley, MN) at locations equidistant both upstream and downstream of the mounted vessel. Average pressure measurements between sensors dictated the motions of the linear actuator during various stages of testing to maintain a set internal pressure. Pressure and force measurements were recorded at 100 Hz, while images of the vessel were taken at 3 Hz using a high-resolution camera (PL-A641, Pixelink, Ottawa, Canada).

After mounting prepared vessels to our testing fixture, a reference length (*L;* corresponding to λ_Z=1.0) was determined followed by preconditioning. *L* was found by observing the length at which the force began to increase while stretching an unpressurized vessel. Vessels were preconditioned by incrementally stretching them to approximately 1.2**L*; at each increment of stretch, the internal pressure was cycled 5 times between 6.7 and 20 kPa.

Vessels were then subjected to a series of axial stretch and pressurization tests. For the pressurization tests, vessel length was held constant at approximately 1.2**L* while the internal pressure was cycled between 6.7 and 20 kPa. For axial stretch tests, internal pressure was held constant at 13.3 kPa (100 mmHg) while vessels were stretched at 0.1 mm/sec between a buckled state and approximately 1.2* *L*. Following pressurization and

axial stretch tests, vessels were stretched axially to failure under constant internal pressure of 13.3 kPa.

Data Analysis

Vessels were assumed to be incompressible, homogenous, circular cylinders with a uniform wall thickness. Cross section measurements were made from top-down images of vessel rings. The zero-load outer diameter (D_e) was determined as the average length of the major and minor axes of the cross section. Reference inner diameter (D_i) was calculated from reference outer diameter (D_e) and cross sectional area (A) (Eq. 1). Average MCA wall thickness was calculated from the difference between reference outer and inner diameters.

$$D_i = \sqrt{D_e^2 - \left(\frac{4A}{\pi}\right)} \qquad \text{Eq. 1}$$

Vessel length was calculated from actuator displacement, and current outer diameter (d_e) was measured from test images in Vision Assistant (National Instruments, Austin, TX). Axial stretch ratio (λ_Z) was defined as the current vessel length (l) divided by the reference length (L) (Eq. 3). Circumferential stretch ratio was calculated as the sum of the current inner and outer diameters (d_i, d_e) divided by the reference inner and outer diameter (D_i, D_e) in Eq. 2.

$$\lambda_\theta = \left(\frac{d_i + d_e}{D_i + D_e}\right) \qquad \text{Eq. 2}$$

$$\lambda_Z = \frac{l}{L} \qquad \text{Eq. 3}$$

The current vessel inner diameter (d_i) was calculated from Eq 4.

$$d_i = \sqrt{d_e^2 - \left(\frac{4A}{\pi\lambda_z}\right)} \qquad \text{Eq. 4}$$

Mean circumferential and axial Cauchy stresses (T_θ, T_z) were calculated as defined in Eqs. 5,6,

$$T_\theta = p_i\left(\frac{d_i}{d_e - d_i}\right) \qquad \text{Eq. 5}$$

$$T_Z = \frac{\lambda_Z}{A}\left(F + \frac{\pi}{4}d_i^2 p_i\right) \qquad \text{Eq. 6}$$

where p_i is pressure and F is force. Force data were postfiltered with a SAE J211 filter, and diameters were interpolated between test images to match corresponding force and pressure data.

Subfailure stiffness values were evaluated from stress–stretch curves generated from the axial stretch and pressurization cycles. An in vivo axial stretch (λ_{Z_IV}) was found during preconditioning and defined as the ratio of vessel length at which axial force did not change during an increase in pressure up to 20 kPa and the reference length. In vivo circumferential stretch (λ_{θ_IV}) was determined from pressurization cycles as the circumferential stretch λ_θ (Eq. 2) at 13.3 kPa. Stiffness values were found by fitting an exponential function to a small segment of the stress–stretch curves (λ_{Z_IV} and λ_{θ_IV} ± 0.01). Stiffness was defined as the value of the derivative of the fitted function evaluated at λ_{Z_IV} and λ_{θ_IV}. Curves having poor fits were excluded from statistical analysis.

A number of parameters were derived from the ultimate failure stress–stretch curves: point of maximum modulus (M_{MAX}, λ_{MAX}), yield point (T_Y, λ_Y), and ultimate point (T_{ULT}, λ_{ULT}) (Figure 3.1). Maximum modulus and yield stress were found by plotting the slope of the curve between every 20th data point. This spacing reduced noise

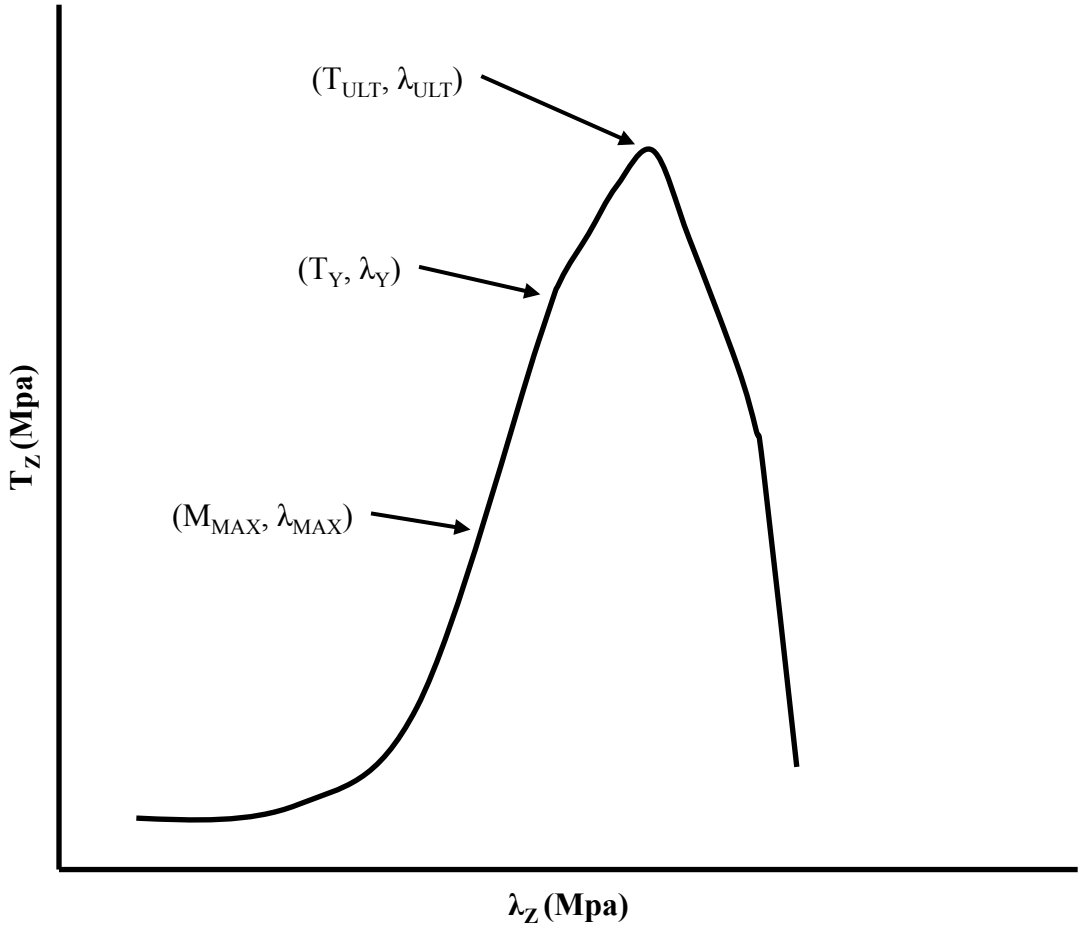

Figure 3.1 Example ultimate failure curve of ovine MCA and general locations of curve parameters: maximum modulus (M_{MAX}, λ_{MAX}), yield point (T_Y, λ_Y), ultimate point (T_{ULT}, λ_{ULT}).

while still representing the behavior of the curve. Maximum modulus was defined as the maximum slope between the toe region and the ultimate stress. Yield stress was defined at the point where the slope decreased 2.347 MPa below the maximum modulus; 2.347 MPa was determined from the average noise amplitude in the plots of the slopes. The ultimate point was determined as the point at which the maximum stress in the failure test was achieved.

Significance of the vessel characteristics between groups was determined using comparison methods with QIMacros for Excel (KnowWare International, Inc. Denver

CO), with a p-value ≤ 0.05 considered significant. Levene's test was first used to determine homogeneity of variance, and where variances were found to be similar ANOVA was conducted, followed by LSD post hoc tests. In cases where homogeneity of variances was violated, Welch's ANOVA test was conducted, followed by Game's Howell post hoc test. In some cases, subfailure stress versus stretch was not obtained. As a result, some analyses do not include a sample size with the aforementioned specimen numbers (11 vessels from each group).

Qualitative Vessel Histology

Untested vessel cross sections were fixed in 4% paraformaldehyde and processed for qualitative histological analysis (ARUP Laboratories, Integrated Oncology and Genetics Services Division, Research Histology, Salt Lake City, UT). Cross sections were embedded in paraffin wax, cut into 3 μm thick sections, and stained with Hematoxylin and Eosin (H&E), Elastica van Gieson (EVG) or Masson's Trichrome stains to identify arterial wall structures. It should be noted that the number of specimens submitted for histology were not sufficient to perform a quantitative analysis of the vessel wall in each age group, but a few general observations were drawn from the available stained sections.

Results

Significant differences in vessel geometry were indicated between nearly all age groups. The average cross-sectional areas (A) increased from 0.117 ± 0.021 mm^2 for the fetal group to 0.378 ± 0.084 mm^2 in the ewe group (Figure 3.2), with significant differences indicated between all groups with exception to the fetal and the newborn

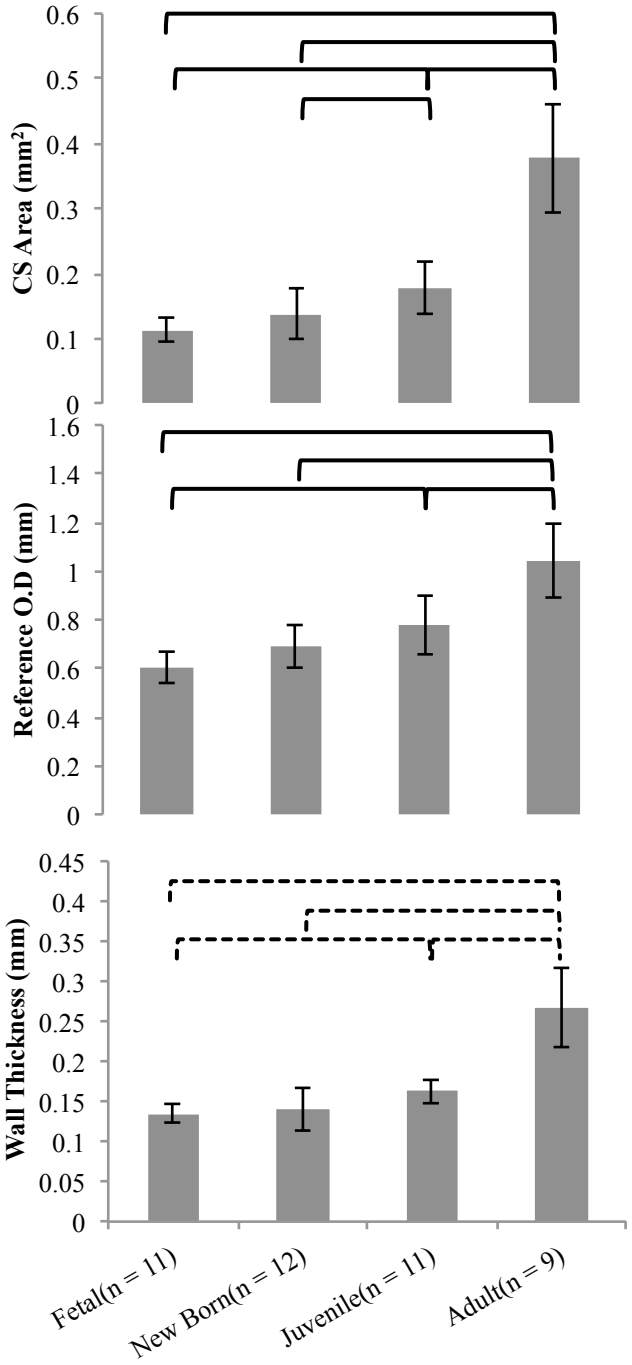

Figure 3.2 Average cross-sectional area, reference outer diameter (O.D), and wall thickness of ovine MCAs. Solid brackets show significance between groups indicated with ANOVA followed by LSD post hoc test. Dashed bars show significance indicated with Welch's ANOVA followed by Games-Howell post hoc test ($p \leq 0.05$).

groups. Similarly, the unloaded outer diameter increased with age from 0.603 ± 0.063 mm in the fetal group to 1.045 ± 0.154 mm in the ewe group, with significant differences between all groups except the fetal and newborn groups and the newborn and juvenile groups. Average MCA wall thickness increased from 0.135 ± 0.013 mm in the fetal group to 0.263 ± 0.047 mm in the ewe group, with significance indicated between all groups with exception to the fetal and newborn groups and the newborn and juvenile groups.

Similar to other biological materials, ovine MCA stress–stretch curves were nonlinear (Figure 3.3). Average subfailure stiffness in the axial direction increased between groups from 0.570 ± 0.336 MPa in the fetal group to 0.802 ± 0.435 MPa in the ewe group. The circumferential subfailure stiffness increased between the fetal (4.479 ± 2.380 MPa) and newborn groups (5.907 ± 2.167 MPa) then decreased from the newborn group to the ewe group (2.776 ± 0.839 MPa); axial subfailure stiffness showed no significance between groups while subfailure stiffness in the circumferential direction showed significance between the fetal and ewe, newborn and ewe, and 3–4 month and ewe groups (Figure 3.4).

Similar to the subfailure curves, the stress–stretch behavior of the ultimate failure curves was nonlinear (Figure 3.5). In all cases, these curves had a characteristic toe region followed by a linear region in which the point of maximum modulus was found. Curves from younger vessels (fetal and newborn) displayed longer toe regions and plateaued as they reached a maximum stress. Curves from older vessels (juvenile and adult) had smaller toe regions and their maximum values approached a sharp maximum followed by a quick decline in stress. Six parameters (Figure 3.6) of the failure curves

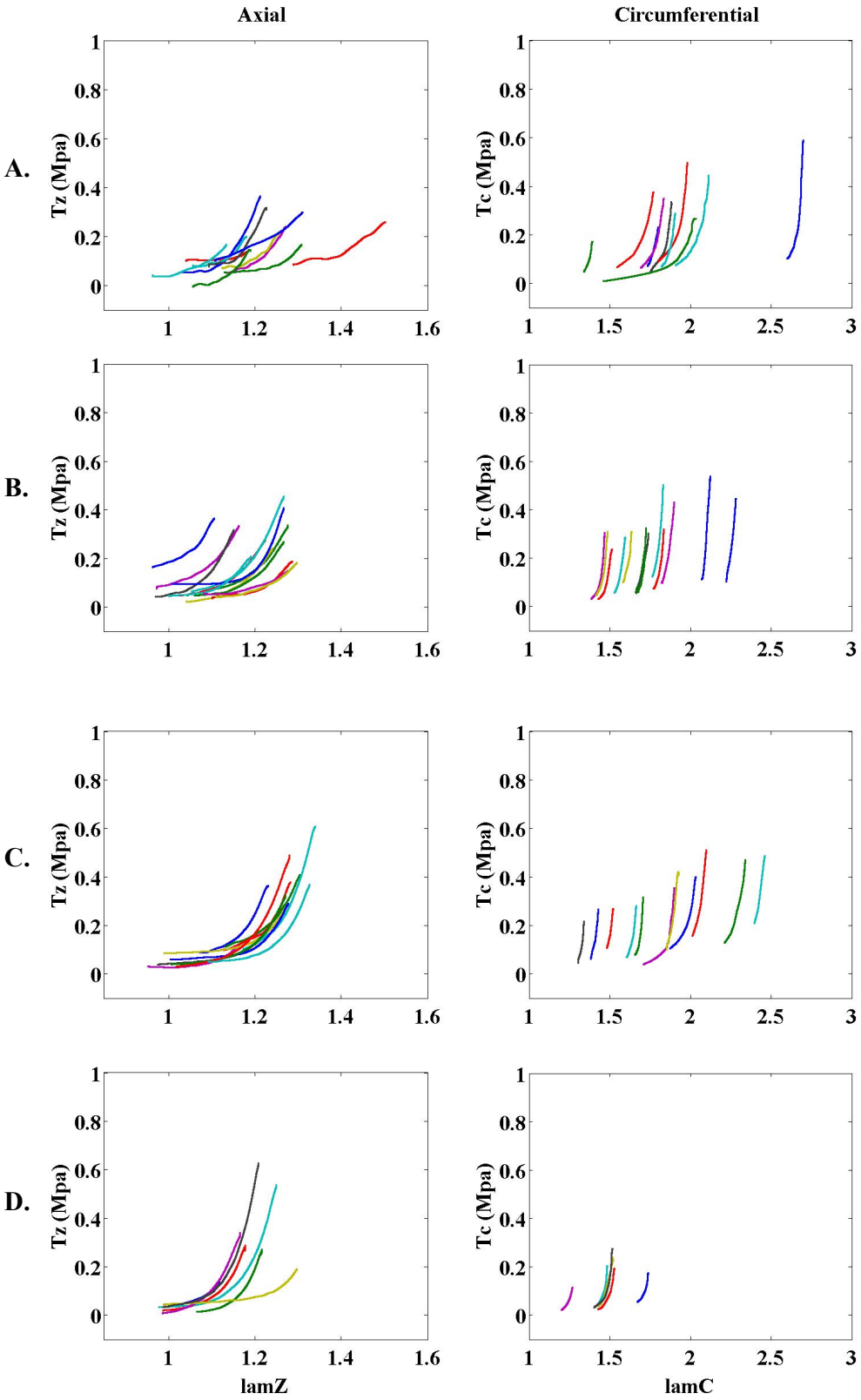

Figure 3.3 Subfailure stress–stretch curves from fetal (row A), newborn (row B), juvenile (row C), and adult (row D) ovine MCA. Colored curves in axial and circumferential plots correspond to the same vessel in each age group.

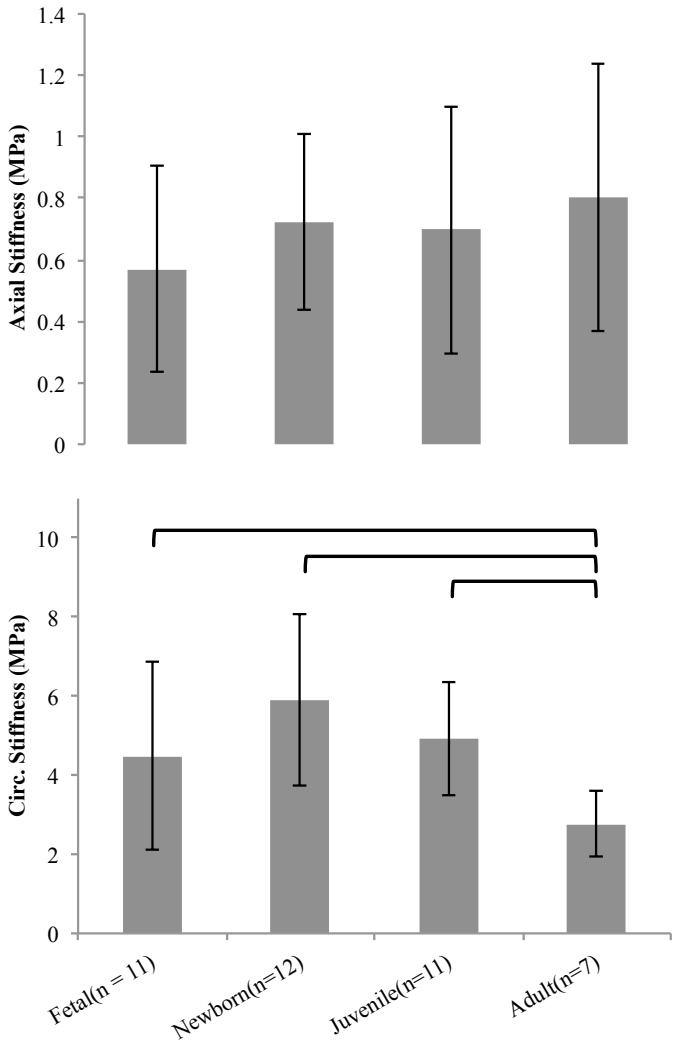

Figure 3.4 Average axial and circumferential stiffness of ovine MCA. Solid bars between groups show significance indicated by ANOVA followed with LSD post hoc test ($p \leq 0.05$). No significance in axial stiffness between age groups was indicated.

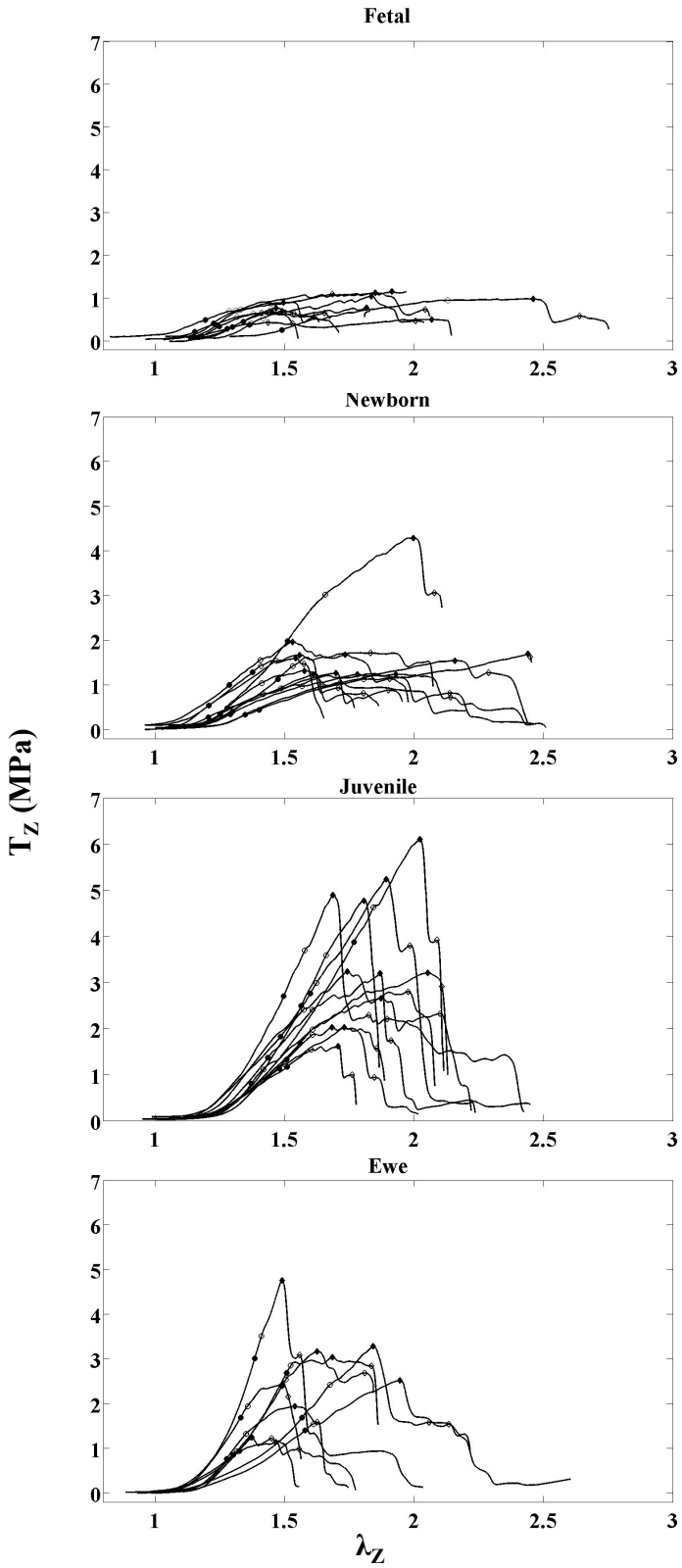

Figure 3.5 Ultimate failure curves of ovine MCA. Failure parameters marked on curves: solid circles indicated maximum modulus, open circles indicate yield point, and solid diamonds indicate ultimate point.

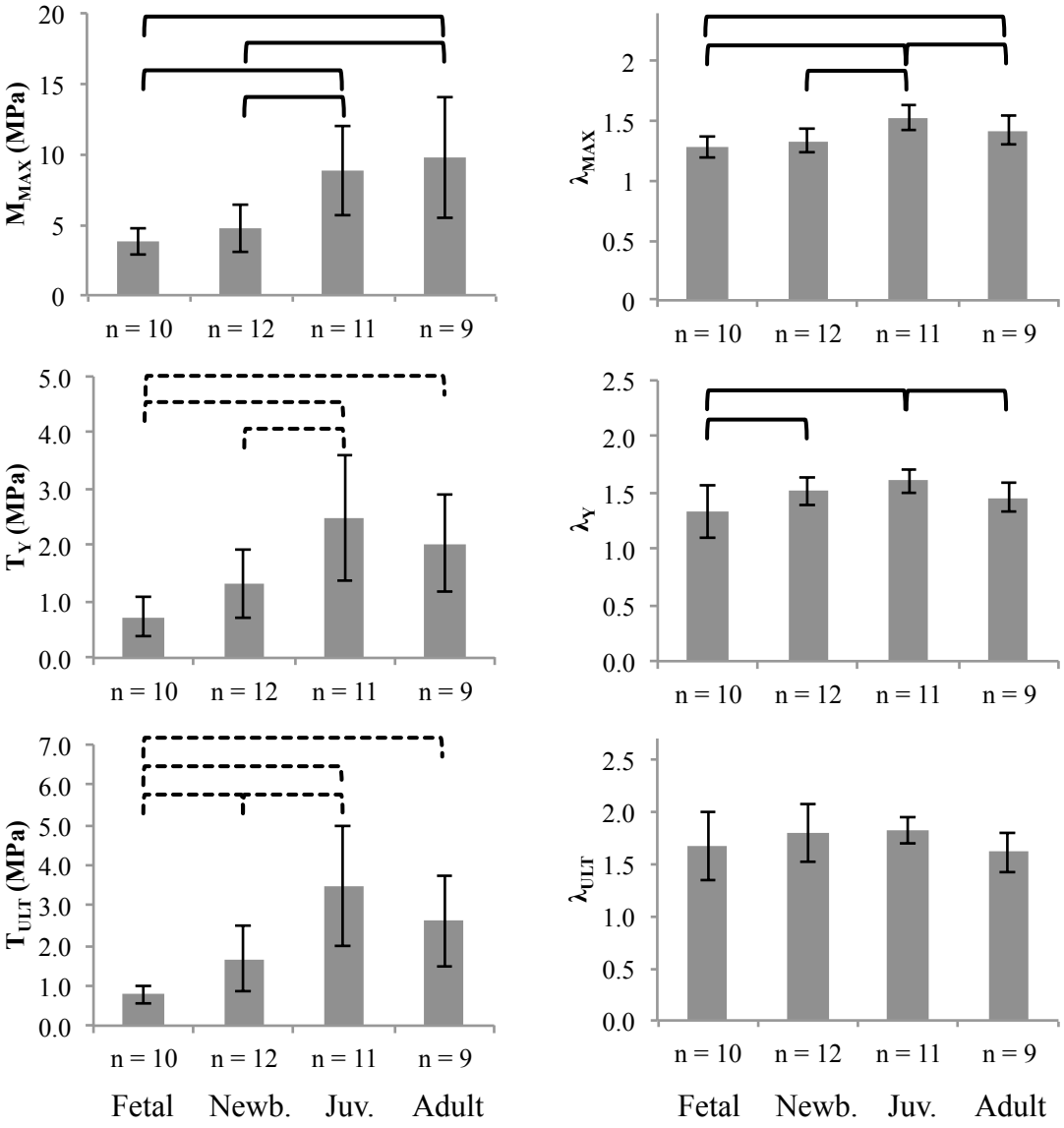

Figure 3.6 Summary of failure parameters for ovine MCA. Solid lines between groups indicate significance by ANOVA and LSD post hoc, dashed lines indicate significance by Welch's ANOVA and Games Howell post hoc test.

were evaluated (M_{MAX}, λ_{MAX}, T_Y, λ_Y, T_{ULT}, λ_{ULT}), and significant differences between groups were found with six of them (M_{MAX}, λ_{MAX}, T_Y, λ_Y, T_{ULT}). Welch's ANOVA followed by Game's Howell post hoc test was used with T_{ULT}, T_Y, while ANOVA followed by LSD post hoc was used with the remaining parameters.

Significant differences were found in M_{MAX} between all groups except the fetal and newborn and the juvenile and the ewe group, while differences were found between the fetal and juvenile, fetal and ewe, newborn and juvenile, and juvenile and ewe groups with the λ_{MAX}. Differences were also found to be significant at T_Y between fetal and juvenile, fetal and ewe, and newborn and juvenile groups, while differences between λ_Y were found with the fetal and newborn, fetal and juvenile, and juvenile and ewe groups. Significant differences in T_{ULT} were found between the fetal group and all other groups, as well as the newborn and the juvenile groups, while λ_{ULT} between groups showed no significance. While comparisons between stresses are considered to be more useful than force measures, it should be noted that there were significant differences between all groups in comparisons of maximum force.

Vessel cross sections stained with H&E, EVG, and Masson's Trichrome indicated differences between age groups. Cell nuclei (blue) and extracellular matrix (pink) are indicated in H&E stain while elastic (dark purple) and collagen (red) structures are visible in EVG stain. Smooth muscle (red) and collagen (blue) are represented in Masson's Trichrome stain (Figure 3.7). Generally, the number of smooth muscle layers increased from fetal to the ewe groups as indicated in the H&E stained sections. Also, the EVG stain indicated a larger ratio of elastic layers to wall thickness in the younger lambs compared to the adults. The smooth muscle content also appeared to be greater in the

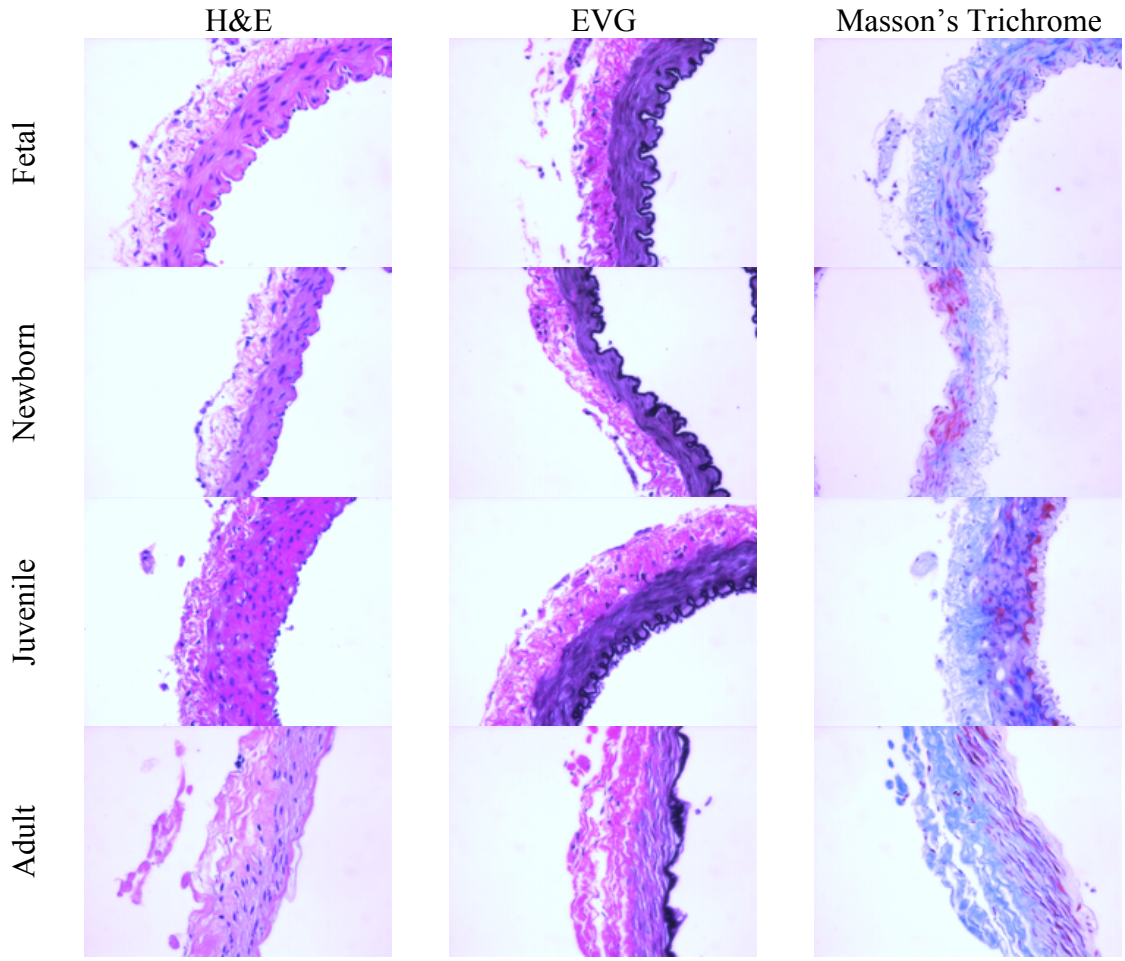

Figure 3.7 Stained sections of ovine MCA at 40X. Pictures represent observations of stained sections in each age group. H&E (left column), EVG (middle column), and Masson's Trichrome (right column) stained sections.

older lambs than in the younger lambs as indicated with the Masson's Trichrome stain.

Discussion

The objective of this study was to compare the mechanical properties of pediatric and adult ovine cerebral arteries taken from subfailure and failure loads. Comparisons of MCA mechanical properties between groups appear to be consistent with our hypothesis that blood vessels from a young population would be more distensible and carry less stress than the older population. Results from both failure and subfailure data indicate an increasing stiffness in the axial direction with age, although differences between groups

with subfailure axial stiffness were not statistically significant. Nearly all parameters measured from failure data showed significance between age groups. Failure curves of left and right vessels from the same animal had similar shapes and values. Stretch values λ_{MAX}, λ_{ULT}, λ_{Y} consistently increased between the younger groups then decreased in the adult group. Interestingly, however, our findings indicate adult vessels carry less maximum stress and yield at lower stresses compared to the juvenile group.

As expected, subfailure stiffness increased with age although not to the level of statistical significance. Applying the average standard deviation and a power of 0.8, it was determined that 340 samples would be required to indicate significance with the subfailure stiffness in the axial direction. The circumferential subfailure stiffness did not follow any expected trends with age. This may be a result of the difference in ovine blood pressures and the pressures used in the subfailure tests; blood pressure of lambs is approximately 30–50 mmHg [18] and 80–90 mmHg in sheep [19]. The difference in test and in vivo pressures, in combination with the nonlinear nature of the stress–stretch curves, may result in higher calculated circumferential stiffness in the younger groups compared to the adult group.

Consistent with the observed changes in mechanical properties, changes in histological characteristics also occurred with age. Stained cross sections indicate that the number of smooth muscle layers increases with age while the thickness of the internal elastic lamina decreases (Figure 3.6). A greater abundance of elastic layer may be responsible for more distensibility in the younger vessels. Collagen is primarily responsible for the stiffness of the artery wall [20], and the apparent proportions of collagen to elastic layer in the adult group may be responsible for its greater stiffness.

Changes in dimensions followed expected trends with increasing age. Younger vessels were smaller in diameter, cross sectional area, and wall thickness than older vessels. Given the adaptiveness of blood vessels to their mechanical environment, a larger diameter and thicker walled artery in older vessels to meet the strains of higher blood pressure is expected.

While the presented data are considered reliable, some limitations in methodology should be noted. The typical in vivo pressure range of lambs is approximately 30–50 mmHg and that of sheep is 80–90 mmHg; therefore the vessels were subjected to supraphysiological pressures in preconditioning and during testing. Our objective was to compare tissue properties between pediatric and adult cerebral vessels, so it was considered reasonable to subject all age groups to a similar loading to allow direct comparisons. However, it should be noted that the imposed supraphysiological pressures did result in slight tissue softening, primarily in the circumferential direction. Softening usually resulted in rightward curve shifts of stretch values between 0.05 and 0.1, while the axial loading behavior was unaffected. Subjecting blood vessels to supraphysiological pressures is not uncommon in the field [21–23]. Another limitation to this study is that stretch values were calculated from actuator displacement rather than tissue fiducial markers, which could lend to higher reported stretch values since axial stretch tends to be higher at the ends where circumferential stretch is constrained [24]. Comparisons between stretch values calculated from microsphere and actuator motion indicate differences between 2 and 10%.

While the ovine brain is a commonly used animal model in the study of brain injuries [25–27] and development [28,29], it is unknown if the presented changing

mechanical characteristics with age are similar in humans. The age range of animals collected in this study corresponds to 32 weeks gestation up to adulthood in humans. Our findings indicate that ovine cerebral vessels become increasingly stiffer in the axial direction with age. Also, the yield and ultimate stress increases from a fetal age up to a juvenile age, then decreases into adulthood. This change occurs between 7 months and 7 years in sheep, which corresponds to puberty to adulthood in humans.

Consistent with previous work [30–32], our findings indicate a stiffening of the cerebral artery with advancing age. However, the mechanical properties of cerebral arteries in the fetal and newborn age range have not been fully investigated. The present findings are also the first to consider the axial loading direction as well as failure level deformations. Although it remains unknown, contrasting mechanical properties of young compared to adult cerebral vasculature may be an underlying cause of the observed differences in symptoms of TBI in children compared to adults. Characterizing age-related changes in the mechanical properties of cerebral vessels could lead to better identification of damage causing loads from TBI and diagnostic and treatment regimes for victims.

References

[1] Faul, M., Xu, L., M., W. M., and Coronado, V. G., 2010, "Traumatic Brain Injury in the United States: Emergency Department Visits, Hospitalizations and Deaths 2002-2006," Centers for Disease Control and Prevention, National Center for Injury Prevention and Control, Atlanta, GA.

[2] Finkelstein, E. A., Phaedra S., and Miller, T. R., 2006, The incidence and economic burden of injuries in the United States, Oxford University Press, New York.

[3] Lindenberg, R., and Freytag, E., 1969, "Morphology of brain lesions from blunt trauma in early infancy," Arch. Pathol., 87(3), pp. 298–305.

[4] Langfitt, T. W., Obrist, W. D., Gennarelli, T. A., O'Connor, M. J., and Weeme, C. A., 1977, "Correlation of cerebral blood flow with outcome in head injured patients," Ann. Surg., 186(4), pp. 411–414.

[5] Armstead, W. M., 1999, "Cerebral hemodynamics after traumatic brain injury of immature brain," Exp. Toxicol. Pathol., 51(2), pp. 137¬142.

[6] Udomphorn, Y., Armstead, W. M., and Vavilala, M. S., 2008, "Cerebral blood flow and autoregulation after pediatric traumatic brain injury," Pediatr. Neurol., 38(4), pp. 225–234.

[7] Huh, J. W., and Raghupathi, R., 2009, "New concepts in treatment of pediatric traumatic brain injury," Anesthesiol. Clin., 27(2), pp. 213¬240.

[8] Cantu, R. C., and Gean, A. D., 2010, "Second-impact syndrome and a small subdural hematoma: an uncommon catastrophic result of repetitive head injury with a characteristic imaging appearance," J. Neurotrauma., 27(9), pp. 1557–1564.

[9] Kochanek, P. M., 2006, "Pediatric traumatic brain injury: quo vadis?," Dev. Neurosci., 28(4–5), pp. 244¬255.

[10] Snoek, J. W., Minderhoud, J. M., and Wilmink, J. T., 1984, "Delayed deterioration following mild head injury in children," Brain, 107 (Pt 1), pp. 15–36.

[11] Bruce, D. A., 1990, "Head injuries in the pediatric population," Curr. Probl. Pediatr., 20(2), pp. 61–107.

[12] DeWitt, D. S., and Prough, D. S., 2003, "Traumatic cerebral vascular injury: the effects of concussive brain injury on the cerebral vasculature," J. Neurotrauma, 20(9), pp. 795–825.

[13] Monson, K. L., Goldsmith, W., Barbaro, N. M., and Manley, G. T., 2003, "Axial mechanical properties of fresh human cerebral blood vessels," J. Biomech. Eng., 125(2), pp. 288¬294.

[14] Monson, K. L., Goldsmith, W., Barbaro, N. M., and Manley, G. T., 2005, "Significance of source and size in the mechanical response of human cerebral blood vessels," J. Biomech., 38(4), pp. 737–744.

[15] Monson, K. L., Barbaro, N. M., and Manley, G. T., 2008, "Biaxial response of passive human cerebral arteries," Ann. Biomed. Eng., 36(12), pp. 2028–2041.

[16] Stemper, B. D., Yoganandan, N., Stineman, M. R., Gennarelli, T. A., Baisden, J. L., and Pintar, F. A., 2007, "Mechanics of fresh, refrigerated, and frozen arterial tissue," J. Surg. Res., 139(2), pp. 236–242.

[17] Bell, E. D., Kunjir, R. S., and Monson, K. L., 2013, "Biaxial and failure properties of passive rat middle cerebral arteries," J. Biomech., 46(1), pp. 91–96.

[18] Unno, N., Wong, C. H., Jenkins, S. L., Wentworth, R. A., Ding, X. Y., Li, C., Robertson, S. S., Smotherman, W. P., and Nathanielsz, P. W., 1999, "Blood pressure and heart rate in the ovine fetus: ontogenic changes and effects of fetal adrenalectomy," Am. J. Physiol., 276(1 Pt 2), pp. H248–256.

[19] Dawes, G. S., Johnston, B. M., and Walker, D. W., 1980, "Relationship of arterial pressure and heart rate in fetal, new-born and adult sheep," J. Physiol., 309, pp. 405–417.

[20] Humphrey, J. D., 1995, "Mechanics of the arterial wall: review and directions," Crit. Rev. Biomed. Eng., 23(1–2), pp. 1–162.

[21] Docherty, C. C., Kalmar-Nagy, J., Engelen, M., and Nathanielsz, P. W., 2001, "Development of fetal vascular responses to endothelin-1 and acetylcholine in the sheep," Am. J. Physiol. Regul. Integr. Comp. Physiol., 280(2), pp. R554–562.

[22] Cox, R. H., 1978, "Comparison of carotid artery mechanics in the rat, rabbit, and dog," Am. J. Physiol., 234(3), pp. H280–288.

[23] Dobrin, P. B., and Rovick, A. A., 1969, "Influence of vascular smooth muscle on contractile mechanics and elasticity of arteries," Am. J. Physiol., 217(6), pp. 1644–1651.

[24] Monson, K. L., Mathur, V., and Powell, D. A., 2011, "Deformations and end effects in isolated blood vessel testing," J. Biomech. Eng., 133(1), p. 011005.

[25] Grimmelt, A. C., Eitzen, S., Balakhadze, I., Fischer, B., Wölfer, J., Schiffbauer, H., Gorji, A., and Greiner, C., 2011, "Closed traumatic brain injury model in sheep mimicking high-velocity, closed head trauma in humans," Cent. Eur. Neurosurg., 72(3), pp. 120–126.

[26] Stubbe, H. D., Greiner, C., Van Aken, H., Rickert, C. H., Westphal, M., Wassmann, H., Akcocuk, A., Daudel, F., Erren, M., and Hinder, F., 2004, "Cerebral vascular and metabolic response to sustained systemic inflammation in ovine traumatic brain injury," J. Cereb. Blood Flow Metab., 24(12), pp. 1400–1408.

[27] Vink, R., Bahtia, K. D., and Reilly, P. L., 2008, "The relationship between intracranial pressure and brain oxygenation following traumatic brain injury in sheep," Acta. Neurochir. Suppl., 102, pp. 189–192.

[28] Finnie, J., Lewis, S., Manavis, J., Blumbergs, P., Van Den Heuvel, C., and Jones, N., 1999, "Traumatic axonal injury in lambs: a model for paediatric axonal damage," J. Clin. Neurosci., 6(1), pp. 38–42.

[29] Finnie, J. W., Blumbergs, P. C., Manavis, J., Turner, R. J., Helps, S., Vink, R., Byard, R. W., Chidlow, G., Sandoz, B., Dutschke, J., and Anderson, R. W., 2012, "Neuropathological changes in a lamb model of non-accidental head injury (the shaken baby syndrome)," J. Clin. Neurosci., 19(8), pp. 1159–1164.

[30] Busby, D. E., and Burton, A. C., 1965, "The effect of age on the elasticity of the major brain arteries," Can. J. Physiol. Pharmacol., 43, pp. 185–202.

[31] Cox, R. H., 1977, "Effects of age on the mechanical properties of rat carotid artery," Am. J. Physiol., 233(2), pp. H256–263.

[32] Le, V. P., Stoka, K. V., Yanagisawa, H., and Wagenseil, J. E., 2014, "Fibulin-5 null mice with decreased arterial compliance maintain normal systolic left ventricular function, but not diastolic function during maturation," Physiol. Rep., 2(3), p. e00257.

CHAPTER 4

SUMMARY

Similar to other biological materials, blood vessels develop and grow to suit the mechanical forces of their environment. As a result of continuous growth and development, the mechanical properties of blood vessels change. Identifying changes in the mechanical properties of blood vessels as they relate to age has the potential to enhance understanding of vascular disease and injury and improve diagnosis and treatment regimes.

Neurological injury or disease as a consequence of blood vessel damage is devastating at any stage in life, but especially in the early, developing years. It is well known that advancing age and disease alter the mechanical properties of blood vessels. However, the mechanical properties of early, developing blood vessels remain ill-defined. Tissue level mechanical tests of blood vessels lend insight into the factors that contribute to alterations in their mechanical properties. Although limitations exist with these types of tissue level testing, they are necessary in developing a complete picture of blood vessel loading behavior.

In this work, the age-related mechanical properties of two types of arteries were investigated: human umbilical artery and ovine middle cerebral artery. The mechanical properties of umbilical arteries were not found to follow any age-related trends in the 24–40 weeks gestation range. Variances of axial and circumferential directions stiffness were

large within groups and significance was undetected. Also, no indication of IVH susceptibility was drawn from the limited number of collected samples. Although the mechanical properties of the umbilical artery did not indicate IVH susceptibility in preterm infants, the full prognostic value of the umbilical cord remains an area of further exploration. Correlations between mechanical properties of the umbilical artery and birth weight, maternal health, or other disorders are possible areas of future research.

Trends in the mechanical properties of the sheep MCA from the fetal age to adulthood were identified through biaxial loading tests and are consistent with previous work. Ultimate and yield stress in the axial direction followed unexpected trends– increasing from the fetal to juvenile age then decreasing in adults. Although in vivo cerebral vessel deformation from traumatic brain injuries and consequent progression of TBI symptoms remain undefined, age-related differences in the mechanical properties of cerebral vessels may be responsible for the symptoms in young compared to old TBI victims. Further identifying age-related differences in cerebral vessel loading behavior would contribute to a better understanding of injury thresholds in TBI victims at all stages of life.